

Effect of Secondary Orientation on the Mechanical Behavior of a Unit Cell Model with a Film-cooling Hole in Single Crystal

Gang Cao, Zhixun Wen, Dashun Liu and Zhufeng Yue

School of Mechanics, Civil Engineering and Architecture, Department of Engineering Mechanics, Northwestern Polytechnical University, Xi'an 710072, PR China

caogang@nwpu.edu.cn

Abstract: A 3D unit cell model with a hole has been set up to analyze the stress and strain distribution near the hole of nickel-based single crystal. The emphasis is placed on the influence of secondary orientation on the mechanical behavior of cell model. The crystallographic slip theory was applied to calculate the elasto-plastic deformation. The results show that, the maximum Mises stress and the maximum resolved shear stress are strongly dependent on the secondary orientation. The minimum plastic strain energy density criterion predicts that the optimal orientation of the hole is $\langle 100 \rangle$ crystallographic orientation. In addition, the secondary orientation has limited influence on the stress distribution near the hole. But the influence of the secondary orientation on the plastic strain energy density distribution around the hole is obvious.

1. Introduction

At present, most single crystal turbine blades are produced by casting with the airfoil stacking direction under control, and the other two orientations are determined but not controlled, named secondary orientation [1]. Therefore, every single crystal blade has a different secondary orientation [2-4]. Recent reviews indicated that secondary orientation has a significant impact on mechanism behavior because the development of the plastic zone at the crack tip is governed by the crystal anisotropy [5,6]. So understanding the stress and strain response in the cooling holes for single crystal turbine blade is a key feature for aero-jet engines and gas turbines manufacturers.

The present work is an attempt to find out the influence of secondary orientation on the stress and strength of cooled turbine blade. In section two, the FEA model (unit cell model) and the secondary orientation will be defined. Crystallographic constitutive model and parameters are given out in this paper. Finally, we will discuss the simulating results and indicate the optimal orientation of the cooling holes to increase the fracture strength of cooled turbine blade.

2. Crystallographic Theory and Cell Model

The resolved shear stress is the component of the traction along the direction of slip and related to the Cauchy stress through orientation tensor as:

$$\tau^{(\alpha)} = \sigma : P^{(\alpha)}. \quad (1)$$



Where $P^{(\alpha)}$ is Schmid factor of slip system α . In the rate dependent crystallographic constitutive model, the shear strain rate on the α -th slip system is assumed to be related to the resolved shear stress $\tau^{(\alpha)}$,

$$\dot{\gamma}^{(\alpha)} = \dot{\gamma}_0^{(\alpha)} \left[\frac{\tau^{(\alpha)}}{g^{(\alpha)}} \right] \left[\left| \frac{\tau^{(\alpha)}}{g^{(\alpha)}} \right| \right]^{m-1} \quad (2)$$

Where $g^{(\alpha)}$ is the reference shear stress, $\dot{\gamma}_0^{(\alpha)}$ is the reference shear strain rate and m is the strain rate sensitivity exponent. For single crystal, the expression of strain energy density $dW / dV = \int_0^{\epsilon_{ij}} \sigma_{ij} d\epsilon_{ij}$ can be written more explicitly as:

$$\left(\frac{dW}{dV} \right)_p = \sum_{\alpha=1}^n \int_0^{\gamma^{(\alpha)}} \tau^{(\alpha)} d\gamma^{(\alpha)} \quad (3)$$

In this paper, all the material parameters are as follows, $E=918300$ MPa, $G=972100$ MPa, $\mu=0.386$, $\dot{\gamma}_0^{(\alpha)}=0.003$, $m=0.02$, $\tau_0=324.9$ MPa, $h_0/\tau_0=1.2$, $\tau_s/\tau_0=1.17$.

A type of cooled turbine blade and the unit cell model are shown in Fig. 1 and Fig. 2, respectively. The cell model is taken from the cooled turbine blade. The dimension of the cell model is 2 mm in length, 2 mm in width and 2 mm in thickness. The radius of the film cooling hole is 0.5 mm. The secondary orientation is defined as the angle of the $[0 0 1]$ orientation relative to the random crystal axis of turbine blade, referred to as α . The definition of α can be seen from Fig. 3.

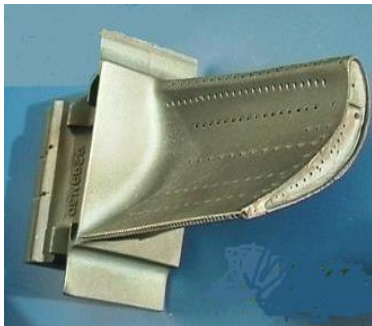


Figure 1. Cooled turbine blade

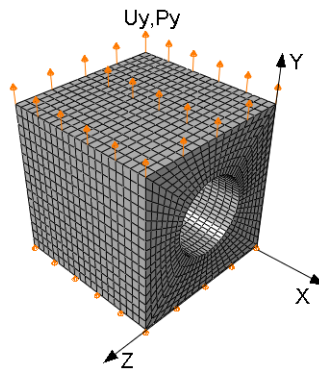


Figure 2. Cell model

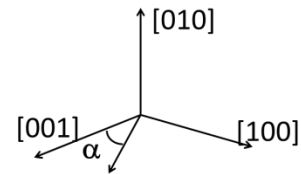
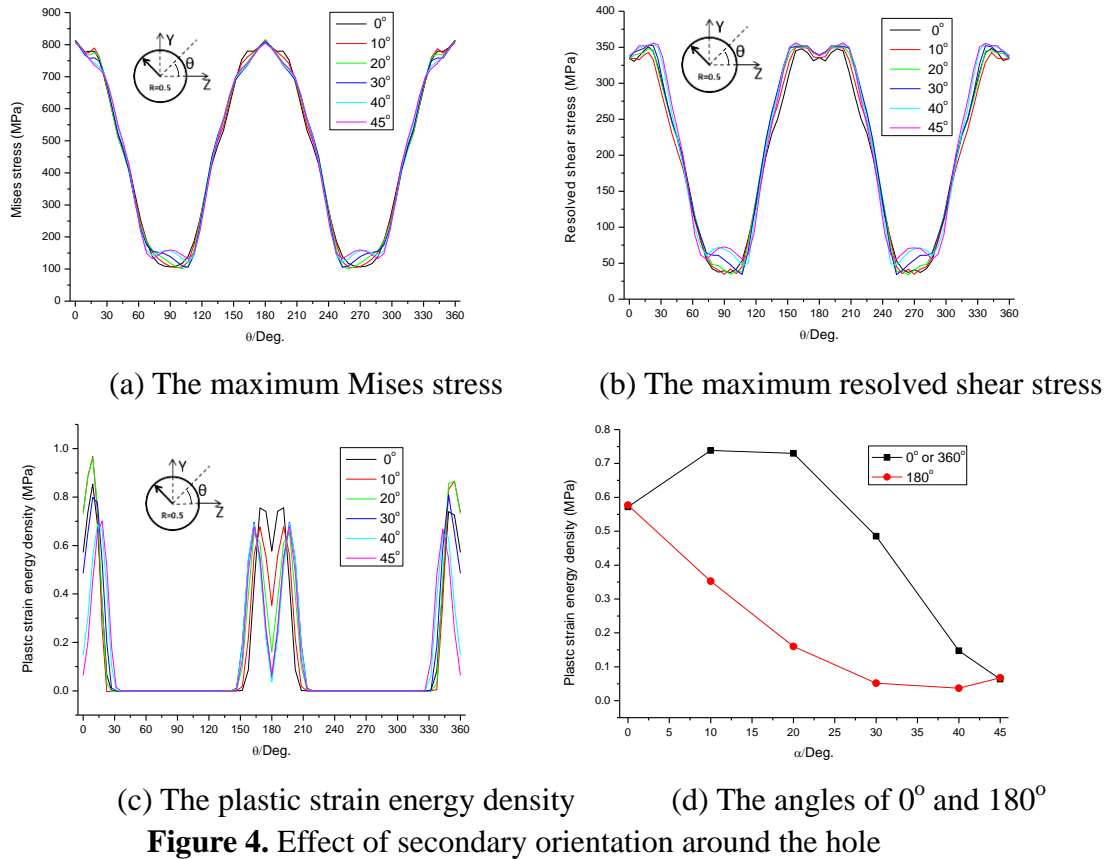


Figure 3. Secondary orientation

3. Mechanical Behavior Near the Hole

Due to the symmetry, the secondary orientation from 0° to 45° is calculated here for simplification. Fig. 4(a)-4(c) show the distribution of Mises stress, maximum resolved shear stress and plastic strain energy density around the hole at the plane $x=-2$ mm, respectively. In different secondary orientations, both the Mises stress and maximum resolved shear stress around the hole present the similar distribution like the letter 'W', as shown in Fig. 4(a) and Fig. 4(b). The Mises stress along the circle angle of 0° and 180° is the largest, while in the circle with the angle of 0° and 270° is the lowest. It is found that the angle with the maximum resolved shear stress is not the same as that the maximum Mises stress locates. The influence of secondary orientation on the Mises stress and the maximum resolved shear stress along the circle is not obvious. But the secondary orientation has obvious influence on the plastic strain

energy density distribution, as shown in Fig. 4(c). Specially, the influence of secondary orientation on the plastic strain energy density at 0° and 180° is remarkable and the change trend is shown in Fig. 4(d). The maximum plastic strain energy density occurs at the circle angles of 0° , $180^\circ \pm 10^\circ$ and 350° . As expected, the plastic strain energy density criterion would predict crack growth to initiate from these places around the cooling hole.



4. Slip Systems Near the Hole

Table 1. Activated slip systems on the surfaces and in the cores of different secondary orientations.

Angle of Secondary orientation	Activated slip systems (strong activation)		Activated slip systems (weak activation)	
	Surface	Core	Surface	Core
0°	2,6,8,10	8,10	3,5,7,12	2,6
10°	2,6,8	8,10	3,5,7,10,12	2,6
20°	2,6	8,10	3,5,7,8,10,12	-
30°	2,3,5,6	8,10	7,8,10,12	-
40°	2,3,5,6	8,10	7,8,10,12	12
45°	2,3,5,6	10,12	7,8,10,12	7,8

The slip system numbered 3, 5, 7 and 12 are not activated at the core, but is weakly active on the surface for secondary orientation $\alpha=0^\circ$. For different secondary orientation α from 0° to 45° , the slip system numbered 3 and 5 are weakly activated on the surface for 0° , 10° and 20° , but is strongly activated for 30° , 40° and 45° . At the core of unit cell hole, the strong activated

slip systems are 8 and 10 except for the secondary orientation 45° , as shown in Table.1. Fig. 5(a) was consistent with the respective slip system number. It can be observed that at the dominant slip field of the core is much more even than that at the surface.

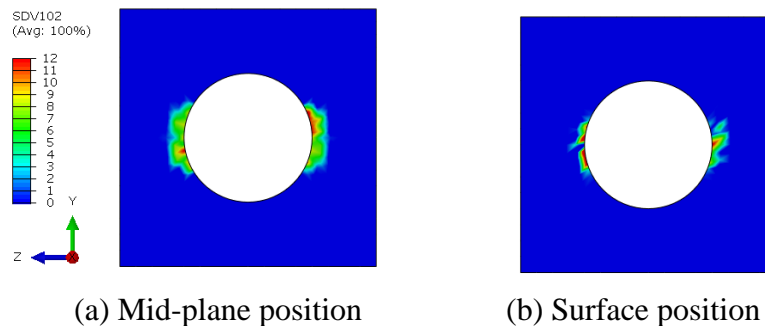


Figure 5. Contours of dominant slip system for secondary orientation

5. Summary

The mechanical response of single crystal with secondary orientation was studied with the cell model by crystallographic FEM. The following summarize are necessary:

1. The distributions of Mises stress and maximum resolved shear stress around the cooling holes are slightly varied with the secondary orientation. But the secondary orientation has obvious influence on the plastic strain energy density distribution around the hole. The initiate cracks occur mainly in the circle with the angle of about 0° and 180° .
2. Comparison between surface and core behaviors, there exist different dominant slip systems and their numbers vary with different secondary orientations.

6. References

- [1] Yiyb J. Kim, S.-M. Kim, Int. J. Heat Mass Transf. Vol.47 (2004), p. 245–256.
- [2] J.E. Nuñez, G. Glinka., Eng. Fract. Mech. Vol.71 (2004), p.1791–1803.
- [3] H.Z. Mao, Z.X. Wen, Z.F. Yue, Mater. Sci. Eng., A Vol.587 (2013), p.79-84.
- [4] Q.M. Yu, Z.F. Yue, Z.X. Wen, Mater. Sci. Eng., A Vol.477 (2008), p.319–327.
- [5] P.A. Sabnis, M. Mazière, S. Forest, Int. J. Plast., Vol.28 (2012), p. 102–123
- [6] D.S. Liu, B.Z. Wang, Z.X. Wen, Adv. Mater. Res. Vol.284 (2011), p.1678-1683.

Acknowledgments

The work was supported by the National Natural Science Foundation of China (51210008, 51375388).